Plastid segregation and cell division in the apicomplexan parasite *Sarcocystis neurona*

Shipra Vaishnava[1], David P. Morrison[1], Rajshekhar Y. Gaji[3], John M. Murray[4], Rolf Entzeroth[5], Daniel K. Howe[3] and Boris Striepen[1,2,*]

[1]Department of Cellular Biology and [2]Center for Tropical and Emerging Global Diseases, University of Georgia, Athens, GA, 30602, USA
[3]Gluck Equine Research Center, Department of Veterinary Science, University of Kentucky, Lexington, KY, 40546, USA
[4]Department of Cell and Development Biology, University of Pennsylvania, PA 19104, USA
[5]Institut für Zoologie, Technische Universität Dresden, Dresden, 01062, Germany
*Author for correspondence (e-mail: striepen@cb.uga.edu)

Accepted 13 April 2005
Journal of Cell Science 118, 3397-3407 Published by The Company of Biologists 2005
doi:10.1242/jcs.02458

Summary

Apicomplexan parasites harbor a secondary plastid that is essential to their survival. Several metabolic pathways confined to this organelle have emerged as promising parasite-specific drug targets. The maintenance of the organelle and its genome is an equally valuable target. We have studied the replication and segregation of this important organelle using the parasite *Sarcocystis neurona* as a cell biological model. This model system makes it possible to differentiate and dissect organellar growth, fission and segregation over time, because of the parasite's peculiar mode of cell division. *S. neurona* undergoes five cycles of chromosomal replication without nuclear division, thus yielding a cell with a 32N nucleus. This nucleus undergoes a sixth replication cycle concurrent with nuclear division and cell budding to give rise to 64 haploid daughter cells. Interestingly, intranuclear spindles persist throughout the cell cycle, thereby providing a potential mechanism to organize chromosomes and organelles in an organism that undergoes dramatic changes in ploidy. The development of the plastid mirrors that of the nucleus, a continuous organelle, which grows throughout the parasite's development and shows association with all centrosomes. Pharmacological ablation of the parasite's multiple spindles demonstrates their essential role in the organization and faithful segregation of the plastid. By using several molecular markers we have timed organelle fission to the last replication cycle and tied it to daughter cell budding. Finally, plastids were labeled by fluorescent protein expression using a newly developed *S. neurona* transfection system. With these transgenic parasites we have tested our model in living cells employing laser bleaching experiments.

Supplementary material available online at
http://jcs.biologists.org/cgi/content/full/118/15/3397/DC1

Key words: chloroplast division, apicoplast, Apicomplexa, cell cycle, parasite, *Sarcocystis neurona*

Introduction

The phylum Apicomplexa represents a large and diverse group of protozoan parasites. Among these are the human pathogens that cause malaria, AIDS-related encephalitis (*Toxoplasma*) and severe enteritis (*Cryptosporidium* and *Cyclospora*). The phylum also contains many parasites of substantial veterinary importance such as *Theileria*, *Babesia*, *Eimeria* and *Sarcocystis*. Aside from their obvious medical and economic importance protozoan parasites have long fascinated cell biologists as model organisms. Recent cell biological work on Apicomplexa has been focused on the cellular structures and molecules involved in their ability to invade mammalian cells, their peculiar cell cycle and mechanisms of cell division, and the presence of several unique organelles. One of these organelles, which has received particular attention, is the apicomplexan plastid or apicoplast.

Given that the cells of the mammalian host lack plastids, the discovery of the apicoplast has provided an entire organelle of potential parasite-specific drug targets. A number of these targets have been validated including several metabolic pathways confined to the plastid, as well as the maintenance of the organelle and its genome (McFadden and Roos, 1999; Ralph et al., 2004). Our interest is focused on apicoplast division and segregation during parasite development. Plastid division is best understood in chloroplasts. Interestingly, chloroplasts still use many elements of their ancestral (cyano-) bacterial division machinery. All plant and algal genomes studied so far harbor two gene families homologous to the bacterial *FtsZ* gene (Miyagishima et al., 2004; Osteryoung et al., 1998; Stokes and Osteryoung, 2003). FtsZ is a prokaryotic homolog of tubulin and the main structural molecule in the bacterial division ring (Lowe and Amos, 1998; Lutkenhaus and Addinall, 1997). Plant FtsZ is targeted to the lumen of the chloroplast where it forms rings at the site of constriction, very much like its bacterial homolog (Kuroiwa et al., 2002; McAndrew et al., 2001; Vitha et al., 2001). Assembly and positioning of this ring is controlled and aided by the homologs of the bacterial cell division proteins MinD and MinE (Colletti et al., 2000; Dinkins et al., 2001; Itoh et al., 2001). In addition to these proteins found in all bacteria, higher plant chloroplasts also employ homologs of Ftn2 and Artemis, which are essential

cell division proteins that are phylogenetically restricted to cyanobacteria (Fulgosi et al., 2002; Vitha et al., 2003). Recently, an eukaryotic element of the division machinery has been identified, a dynamin-like protein that forms a ring on the cytoplasmatic side and is required for proper organellar fission (Gao et al., 2003; Miyagishima et al., 2003). Surprisingly, our extensive comparative genomic analysis of the completed or nearly completed genomes of several plastid-harboring apicomplexan parasites (*P. falciparum*, *P. yoelii*, *T. gondii*, *Eimeria tenella* and *Theileria annulata*) did not identify a single homolog for any member of this conserved machinery. This is despite the fact that several proteins such as FtsZ are highly conserved and readily identified by BLAST search in the genomes of a diverse set of plants and algae (V.S. and B.S., unpublished data).

How is plastid division accomplished in apicomplexan parasites in the absence of the conserved machinery? Previous work on *Toxoplasma* has shown these organisms to employ a genuinely eukaryotic mechanism. Specifically, the dividing plastid associates with the centrosomes of the mitotic spindle (Striepen et al., 2000). As a result of this association the ends of the plastid are inserted into the budding daughter cells and segregated. Based on the observation that all Apicomplexa have lost the bacterial machinery, we hypothesized that centrosome association might be the conserved mechanism for apicoplast division. However, there is surprising morphological diversity among plastids in different species of Apicomplexa. While *T. gondii* maintains a small ovoid organelle, other apicomplexans harbor plastids that form complex highly branched structures [e.g. *Plasmodium* (Waller et al., 2000)] or long tubules (*Sarcocystis*, this study). We hypothesize that these morphologies are consistent with the centrosome association model and reflect the diversity of the apicomplexan cell division mechanisms. All lytic cycles in Apicomplexa start and end with a conserved motile stage, which is endowed with a set of organelles required for host cell attachment and invasion (Sibley, 2004). However, the development within the host cell and the underlying cell cycle model vary dramatically between closely related species and even between different life cycle stages of the same organism. In addition to more conventional models, Apicomplexa can forego cytokinesis and/or nuclear division for several cell cycles yielding multinucleate or polyploid stages that finally give rise to multiple daughter cells.

We have tested this hypothesis using the apicomplexan *Sarcocystis neurona* as a new cell biological model. *S. neurona* is the causative agent of equine protozoal myeloencephalitis (Dubey et al., 2001; Lindsay et al., 2004). This parasite can be maintained in tissue culture continuously, and its developmental stages are relatively large, permitting high resolution imaging in infected cells. Furthermore, the peculiar *S. neurona* cell division mechanism dissociates DNA replication, nuclear division and cytokinesis over an extended period, thereby providing a unique system to dissect the relationship of plastid maintenance, fission and segregation with mitosis and cytokinesis. In this study we demonstrate that *S. neurona* undergoes five cycles of chromosome replication without nuclear division. Interestingly, intranuclear spindles persist throughout the cell cycle providing a potential mechanism to organize chromosomes and organelles in an organism with a polyploid nucleus. By using molecular markers and pharmacological treatments we show that centrosomes and spindles are essential for plastid organization and faithful segregation. The timing and mechanism of organellar fission was also analyzed. Finally, a transfection system was established for this organism to validate the model in vivo through live cell microscopy and laser bleaching experiments.

Materials and Methods

Host cells and parasites

Sarcocystis neurona strain SN3 was propagated in primary bovine turbinate (BT) cells. BT cells were grown in Dulbecco's modified Eagle's medium (DMEM, HyClone) supplemented with 10% heat-inactivated fetal bovine serum (HyClone), 2 mM L-glutamine, 5 U/ml penicillin, 10 μg/ml streptomycin, and 1 ml/l fungizone (Invitrogen). A continuous culture was maintained by weekly passage of 1 ml culture supernatant containing *S. neurona* merozoites into a fresh BT culture. We have noticed (as have others) that inefficient parasite egress from the host cell seems to limit the number of infective parasites that can be obtained (Ellison et al., 2001). In some experiments infected cultures were scraped after 72 hours and forced through a 26 1/2 gauge needle to break host cells. Free parasites were purified by filtration through 3 μm polycarbonate membrane (Costar) prior to infection of cell cultures.

A stable transgenic *Toxoplasma gondii* strain expressing the reporter ferredoxin NADH reductase-red fluorescent protein (FNR-RFP) was established and cultivated in human foreskin fibroblast (HFF) cells as previously described (Striepen et al., 2000).

S. neurona transfection

Plasmids for *S. neurona* transfection experiments were initially derived from the *T. gondii* expression vector *p*tubYFP-YFP/sagCAT (Gubbels et al., 2003; Striepen et al., 2000) by replacement of the *Toxoplasma* tubulin promoter and the selectable marker cassette with the 5′ flanking region of the *S. neurona* SAG1 locus (Howe et al., 2004); R.Y.G., V.S., B.S. and D.K.H., unpublished data). To engineer the plastid reporter construct *p*SnsagFNR-RFP used in this study, the coding region of FNR-RFP along with the 3′ UTR derived from the *T. gondii* DHFR-TS gene was excised from plasmid *p*tubFNR-RFP (Striepen et al., 2000) with *Not*I and *Bgl*II and ligated into *p*SnsagYFP-YFP digested with *Not*I and *Bgl*II, placing the transgene under the control of the *S. neurona* promoter. The coding sequence of the *T. gondii* acyl carrier protein was excised for plasmid *p*tubACP-GFPsagCAT (Waller et al., 1998) using *Bgl*II and *Avr*II and was ligated into *p*SnsagYFP-YPF equally restricted to replace the first YFP cassette to yield pSnsagACP-YFP.

Freshly lysed *S. neurona* merozoites were purified by filtration through 3 μm polycarbonate filters and resuspended in cytomix (120 mM KCl, 0.15 mM $CaCl_2$, 10 mM K_2HPO_4/KH_2PO_4 pH 7.6, 25 mM Hepes pH 7.6, 2 mM EDTA, 5 mM $MgCl_2$, 2 mM ATP, 5 mM glutathione) to a density of 3×10^7 parasites per ml. 50 μg plasmid DNA were ethanol precipitated, resuspended in 100 μl cytomix, mixed with 300 μl parasites in a 2 mm electroporation cuvette, and exposed to a 1800 V, 25 Ω and 25 μF pulse generated by a BTX ECM 630 apparatus (Genetronix).

Fluorescence microscopy

For immunofluorescence, filter-purified *S. neurona* merozoites were allowed to settle for 10 minutes on polylysine-coated coverslips (coverslips were pretreated for 20 minutes with 10 mg/ml polylysine, washed and air dried). Alternatively, BT cells were grown to confluency on sterilized glass coverslips in six-well plates and subsequently infected with *S. neurona* merozoites. Cultures were fixed at various

times post-infection for 10 minutes using 4% paraformaldehyde in PBS, followed by permeabilization with 0.25% (w/v) Triton X-100 in PBS. The following primary antibodies were used at the indicated dilutions: affinity purified polyclonal rabbit antiserum against *T. gondii* acyl carrier protein [ACP; 1:400; kindly provided by G. I. McFadden, University of Melbourne (Waller et al., 1998)], monoclonal antibody 12G10 raised against α-tubulin (1:25; kindly provided by J. Frankel, University of Iowa (Jerka-Dziadosz and Frankel, 1995; Jerka-Dziadosz et al., 1995)], monoclonal mouse and polyclonal rabbit anti-centrin [1:400; kindly provided by J. L. Salisbury, Mayo Clinic (Paoletti et al., 1996)], rat polyclonal anti-SnMic10 (Hoane et al., 2003) and rabbit polyclonal anti-IMC3 (Gubbels et al., 2004). All antibodies were diluted in PBS plus 1% BSA and detected using Alexa Fluor 488- or Alexa Fluor 546-conjugated goat anti-mouse, anti-rabbit or anti-rat antibodies (Molecular Probes). DNA was stained by incubation with 2 μg/ml 4′,6′-diamino-2-phenylindole (DAPI; Molecular Probes) for 10 minutes, excess dye was removed by washing, and coverslips were mounted with Gel/Mount (Biomeda Corporation). Fluorescence images were captured with a CCD camera (C4742-95; Hamamatsu) on a Leica DMIRBE microscope. Image acquisition, contrast adjustment and channel merging were performed using openlab software (Improvision).

To estimate the DNA content of individual schizont nuclei, the intensity of DAPI staining was measured in situ by image analysis. Fixed cultures were stained for tubulin and DNA as described above. Images were collected in the red and DAPI channel with constant exposure time and within the linear range of the CCD camera (the contrast was not adjusted). Nuclei were defined as objects by generating binary image masks for each image using a thresholding function. The mean (background-subtracted) pixel intensity was multiplied by the area of each nucleus to obtain a cumulative intensity measurement in arbitrary units. Host cell nuclei were measured as internal controls and provided results consistent with a confluent monolayer mostly arrested in G1 (the bulk of the measurements clustered around a mean of 7.5 10^6 units Std 1.2 10^6, n=20), and two cells with 12 and 16.5 10^6 units, probably representing G2 and S phase, respectively.

Laser bleaching experiments

For deconvolution microscopy and laser bleaching experiments confluent BT and HFF coverslip cultures were infected with transgenic FNR-RFP-expressing *S. neurona* and *T. gondii,* respectively. Cultures were observed on a Delta Vision Spectris deconvolution workstation (Applied Precision) with an Olympus 60× NA 1.2 water immersion lens 48 hours after transfection. Coverslips were mounted in medium (Secure-Seal, Molecular Probes) and maintained at 37°C during the observation. A 25 mW argon laser was used to bleach the sample, by exposing it to five 488 nm pulses for 300 mseconds each at 1.5 mW laser power. The size of the laser spot was nominally diffraction limited. Stacks of optical sections were taken before and after the bleach with z-increments of 0.3 μm and xy spacing of 0.1 μm. The pre- and the post-bleach images were set to identical contrast setting using the image-scaling function in the Softworx software (Applied Precision). Total projection images of sequential *z*-stacks were rendered using Volocity software (Improvision).

Drug treatment

The dinitroaniline herbicide oryzalin was obtained from Riedel-deHaen (Seelze, Germany), and a 10 mM stock solution was prepared

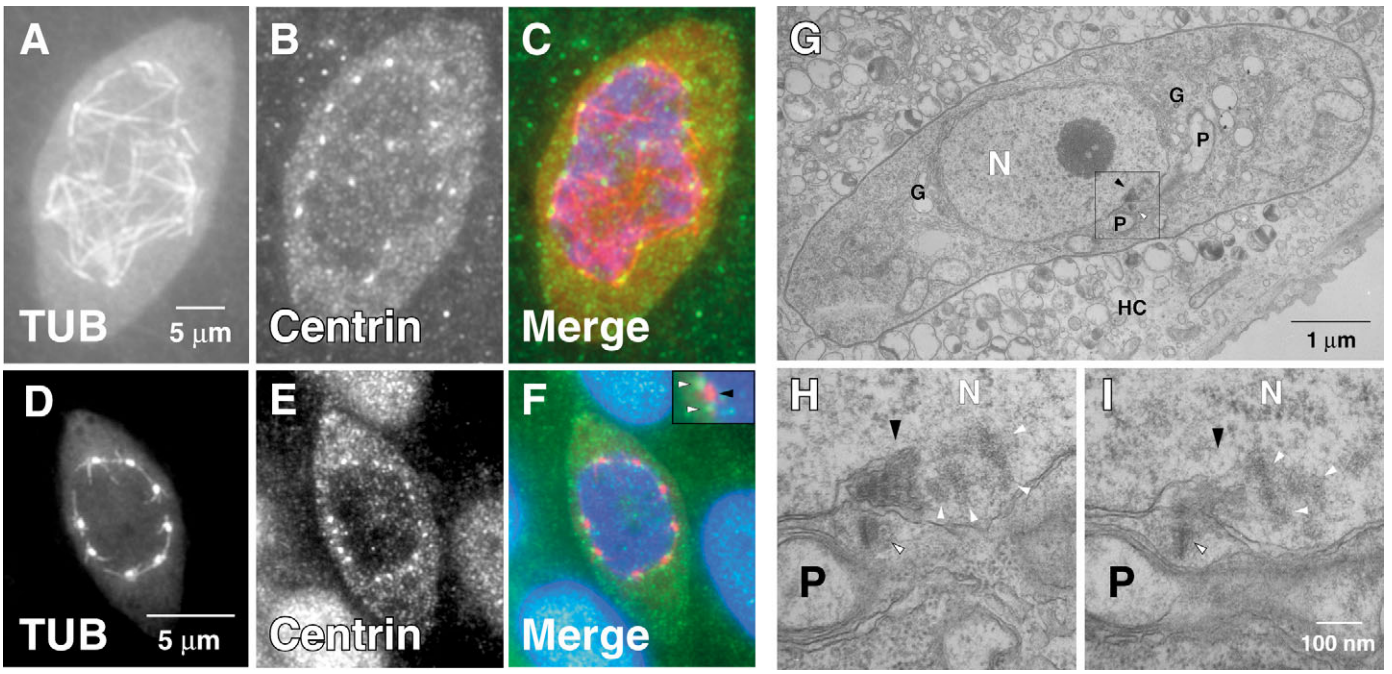

Fig. 1. Short intranuclear spindles are maintained throughout the cell cycle. *S. neurona*-infected cultures were double labeled with anti-tubulin (A,D) and anti-centrin (B,E) antibodies to detect microtubules and centrosomes, respectively. (C,F) The merged images of the red (tubulin), green (centrin) and blue (DAPI) channels. Centrosomes organize a complex network of spindle microtubules during mitosis (A-C). The 'dots' of tubulin staining observed during interphase are flanked by two centrosomes (D-F, also see inset in F). (G-I) *S. neurona*-infected cultures were fixed in situ, embedded in Epon and ultrathin sections were cut for electron microscopy. (G) A section through a young schizont. The nucleus (N) is located at the center of the cell and plastid (P) and Golgi (G) are equally discernible. (H,I) Serial sections of the boxed region of G at higher magnification. A short basket of microtubules is evident within the nucleus (black arrowhead), which emanates from a centrosome on the cytoplasmatic site of the nuclear envelope (white arrowheads with black outline). Interestingly the end of this minute spindle seems to be in contact with condensed nuclear material (white arrows).

in DMSO. Confluent BT cell coverslip cultures were infected with *S. neurona*, allowed to develop for 36 hours, and then treated with 2.5 μg/ml oryzalin for either 24 hours or 48 hours prior to processing for immunofluorescence analysis.

Electron and immunoelectron microscopy

BT cells were grown to confluency in polystyrene Petri dishes and infected with *S. neurona* merozoites. Cells were fixed in situ, 72 hours post infection, with 1% glutaraldehyde and 1% OsO_4 in 50 mM sodium phosphate buffer pH 7.2 for 1 hour on ice, followed by overnight staining with 0.5% aqueous uranyl acetate. Samples were dehydrated using a progressive ethanol series, ethanol was gradually exchanged for resin and samples were embedded in EPON (Electron Microscopy Sciences) directly in the dish. Blocks of polymer were cut from the dishes and ultrathin sections were taken parallel to the monolayer using a diamond knife. Sections were placed on Formvar-coated grids, stained with 4% uranyl acetate and 4% lead citrate and observed using a JEO JEM-100 CX II microscope.

For immunoelectron microscopy, infected cells were fixed with 2% paraformaldehyde and 0.1% glutaraldehyde in 0.5× PBS for 20-30 minutes on ice. Fixed cells were washed, scraped and centrifuged. The pellet was progressively dehydrated with ethanol and gradually infiltrated with LR-White on ice. Finally the sample was transferred to a gelatin capsule and polymerized at 50°C. Ultrathin sections cut from trimmed blocks and recovered on Formvar-coated grids were placed on 50 μl drops of the polyclonal anti-ACP antibody (1:400 in PBS 2% BSA) followed by 1:50 goat anti-rabbit IgG conjugated with 10 nm gold (BBinternational). After immunolabeling, sections were stained and analyzed as described above.

Results

Successive rounds of synchronous mitosis give rise to a polyploid parasite

*Sarcocysti*s is an obligate intracellular parasite. After invasion of the host cell, the parasite develops over 2-3 days during which the nucleus seems to grow continuously until it fragments into multiple nuclei, which are packaged into daughter cells (Speer and Dubey, 1999; Speer and Dubey, 2001). We have followed these events by fluorescence microscopy using *S. neurona*-infected tissue cultures as a model. The schizonts are lemon shaped and lie directly within the host cells cytoplasm. Their central large nuclei were intensely stained by the DNA intercalating dye DAPI (Fig. 1). Using a monoclonal antibody raised against α-tubulin from *Tetrahymena thermophila* (Jerka-Dziadosz and Frankel, 1995), we observed only moderate and diffuse staining in the parasite cytoplasm. This is in agreement with the previous reports that schizonts lack subpelicular microtubules, which are characteristic of the invasive stages of Apicomplexa (Morrissette and Sibley, 2002a). Within the nucleus however, two consistent and mutually exclusive staining patterns were observed: multiple intranuclear bundles of microtubules, or intensely stained dots right under the nuclear envelope (Fig. 1A,D). The microtubule bundles seemed to emanate from points close to the surface of the nucleus and coincided with apparent condensation of the DNA staining. This suggests that they represent mitotic spindles, segregating chromosomes (Speer and Dubey, 1999). To confirm this finding, infected cultures were double labeled with the anti-tubulin antibody and an anti-centrin serum. Centrin is a cytoplasmatic calcium binding protein that is concentrated in centrosomes surrounding the centrioles (Salisbury, 1995). This serum has previously been shown to label the centrosomes in the related parasite *T. gondii* (Striepen et al., 2000). As shown in Fig. 1C-F, the poles of these spindles clearly coincided with the centrin label. Note that the multiple centrosomes are linked by individual microtubules that span across the nucleus.

Short intranuclear spindles are maintained throughout the cell cycle

The staining patterns observed for the mitotic spindles were often too complex to count their numbers unambiguously. The dots in the second staining pattern however, could be easily counted and their number increased in geometric progression (2, 4, 8, up to 64; Fig. 2A-F, note that the dot often consists of two very close and poorly resolved structures). The increase in

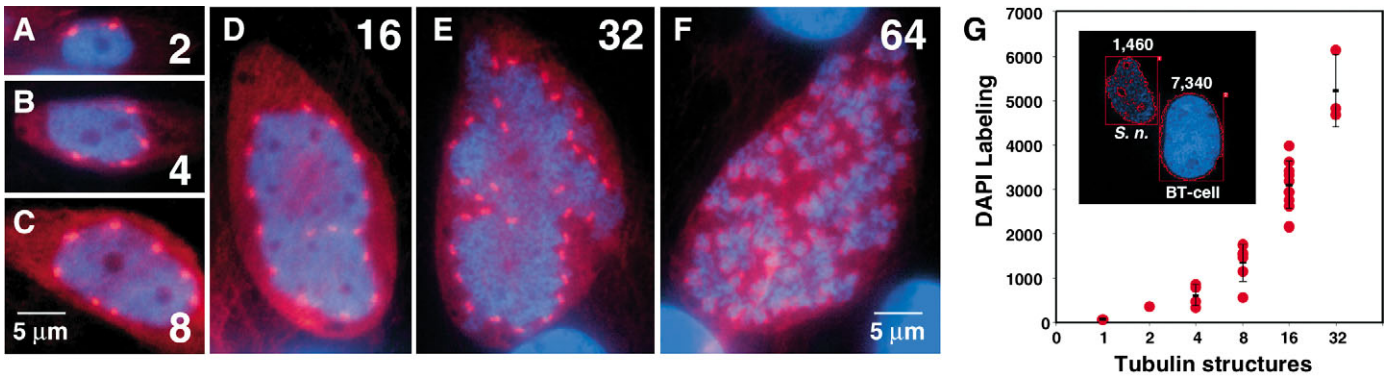

Fig. 2. *S. neurona* forgoes nuclear division and cytokinesis for five cell cycles prior to the budding of 64 daughter cells. Cell cultures were infected with *S. neurona* merozoites and fixed and processed for immunofluorescence 24-72 hours after infection. Cells were incubated with a monoclonal antibody against α-tubulin (red) and DAPI to stain DNA (blue). Developing schizonts present two mutually exclusive staining patterns: multiple spindles throughout the nucleus coinciding with DNA condensation or dots in proximity to the nuclear envelope (see Fig. 1). The number of these dots increased with the size of the schizont in a geometric progression (2-64, A-F). (G) Plot of the intensity of DNA staining of each nucleus (in arbitrary units, as shown for a parasite and host cell nucleus in inset) against the number of tubulin dots per nucleus (100 random fields were analyzed, individual measurements are shown as red dots, black lines and error bars indicate the mean and standard deviation, respectively). Progression from 32 to 64 (E,F) produces 64 daughter nuclei. Note that the dots often appeared as doublets (D).

the number of these structures seemed to be directly correlated with the size of the nucleus. To quantify this relationship, the DNA content of individual nuclei was measured by image analysis. Schizont nuclei were defined using a binary mask (see Material and Methods for detail) and the cumulative intensity of their DAPI label was recorded for each mask. Fig. 2G shows such measurements for nuclei analyzed from 100 fields plotted against the number of tubulin dots recorded for each respective nucleus. The DNA content of schizont nuclei is clearly correlated with the number of dots and as might be expected doubles synchronously with the former indicating that these dots might be associated with or represent minute spindles. Upon double labeling with centrin antiserum, each red tubulin dot was flanked by two green centrosomes (Fig. 1D-F, see inset in F). To further investigate the nature of these structures, infected cultures were fixed and embedded for electron microscopy. Fig. 1G shows a section through a young schizont (the large central nucleolus and the homogenous chromatin structure suggests that this cell is in interphase). Consistent with immunofluorescence images, the electron micrographs demonstrate short baskets of microtubules within the nucleus (Fig. 2H,I, black arrowheads). These microtubules emanate from centrosomes (white arrowheads with black outline), which lie outside of the nuclear envelope in the cytoplasm. As many as 32 of these short spindles were observed associated with a single polyploid nucleus. In even later developmental stages, the nucleus is segregated into 64 daughter nuclei following the last chromosomal duplication event (Fig. 2F). Our analysis concludes that all stages in the developing schizont present either typical spindles (associated with mitosis and DNA condensation), or short interphase spindles. We failed to observe stages devoid of microtubular structures in the nucleus.

The plastid is maintained as a single organelle throughout the intracellular development

To identify the plastid in *S. neurona* and to follow its fate through development, parasites were analyzed by immunofluorescence using a polyclonal antibody raised against *T. gondii* acyl carrier protein (ACP). ACP is a nuclear-encoded protein that is posttranslationally targeted to the lumen of the apicoplast where it takes part in type II fatty acid synthesis. ACP has been previously used as a plastid marker in *T. gondii* and *P. falciparum* (Striepen et al., 2000; Waller et al., 1998; Waller et al., 2000). Extracellular *S. neurona* merozoites stained with this antibody yielded a pattern indistinguishable from *T. gondii* tachyzoites indicating that the antibody cross reacts and recognizes ACP from *T. gondii* as well as *S. neurona* (Fig. 3A-D). The antibody labeled a single small ovoid organelle located apically of the nucleus in extracellular merozoites of *S. neurona*, and staining coincided with a spot of extranuclear DAPI staining representing the plastid genome. This extranuclear DNA hybridized with DNA probes specific for the *S. neurona* plastid genome (V.S. and B.S., unpublished). In developing *S. neurona* schizonts, however, the ACP antibody labeled a single tubular structure (Fig. 3E). Costaining with DAPI revealed that this elongated tubular plastid was associated with the periphery of the nucleus (Fig. 3H). The tubular morphology of the plastid was maintained throughout the intracellular development of the parasite, and no differences were observed between parasites undergoing mitosis and those in interphase (data not shown).

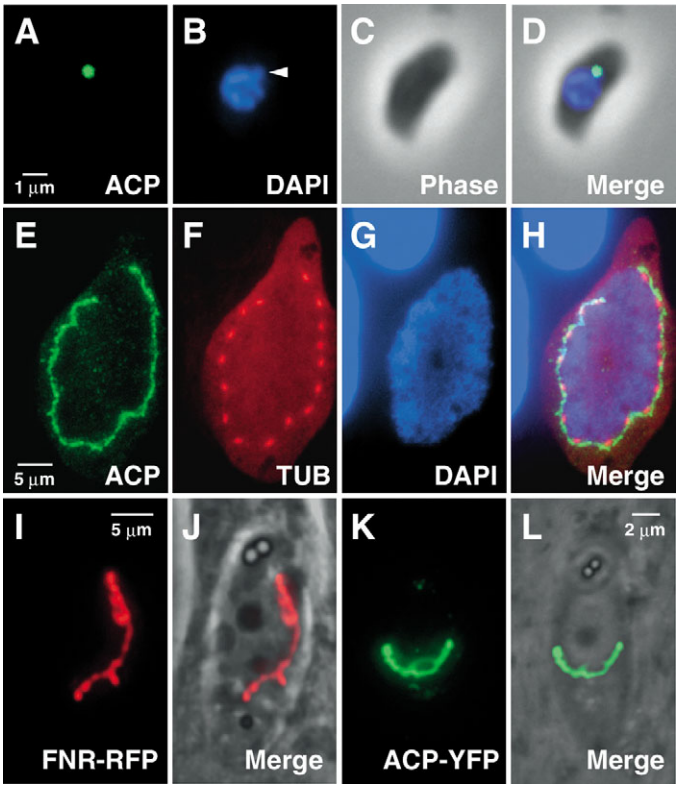

Fig. 3. The plastid in *S. neurona* schizonts is a single tubular structure in close association with the nucleus and its spindles. Extracellular *S. neurona* merozoites (A-D) were fixed and incubated with an affinity-purified rabbit antiserum raised against the *T. gondii* plastid protein ACP (A) and DAPI (B). A single round organelle was detected close to the nucleus colocalizing with the extranuclear plastid DNA (arrowhead). *S. neurona*-infected cultures were fixed 48 hours post-infection (E-H), and simultaneously incubated with antibodies against ACP (green, E), α-tubulin (red, F) and DAPI (G). The plastid in developing schizonts appeared to be a single tubule wrapped around the nucleus (H). (I-L) Transfection plasmids were constructed that place the genes of two plastid targeted proteins from *T. gondii* (FNR and ACP, fused to RFP (red) or YFP (green), respectively) under control of a *S. neurona* promoter element. Plasmids were introduced into *S. neurona* merozoites by electroporation prior to infection. Transformed cultures were observed by fluorescence microscopy in living cells 36 hours after transfection.

In vivo laser bleaching studies confirm a continuous plastid

The presence of a large continuous plastid is highly interesting as it mirrors the development of the nucleus in *S. neurona* and could lend additional support to the model that nucleus and plastid are organized and segregated by the same molecular machinery. Whether the plastid is indeed continuous could not be concluded with certainty based on immunofluorescence analysis, since some samples seemed to show small breaks in the plastid tubule depending on fixation conditions. To avoid fixation artifacts, we developed a transfection system for *S.*

neurona to establish fluorescent-protein-expressing parasites for in vivo analysis (R.Y.G., V.S., B.S. and D.K.H., unpublished). Transfection vectors were constructed with the promoter region of the *S. neurona* SAG1 gene, driving the expression of a reporter gene. The gene for two well-characterized *T. gondii* plastid-targeted proteins (ACP and FNR) were translationally fused to YFP or RFP, respectively. Parasites transfected with these plasmids by electroporation were used to infect coverslip cultures. Images were taken 24-36 hours after transfection without fixation. Transfection with both of these independent reporters resulted in fluorescent labeling of a tubular organelle in close association with the nucleus (Fig. 3I-L).

S. neurona plastids, imaged in vivo, appeared continuous and showed no obvious breaks (see three-dimensional reconstruction derived from deconvolved serial optical z sections in Fig. 4E and Movie 1 in supplementary material). To directly test for organellar continuity, laser bleaching experiments were performed. Given the high rates of diffusion over the small cellular distances, exposure of the distal end of the organelle to a series of laser pulses should bleach fluorescence in the entire organelle. If the organelle is discontinuous, bleaching should remain partial (see Fig. 4A,B for a schematic outline of the experiment). A series of short exposures to the 488 nm laser line at modest power settings was applied to one end of a plastid labeled in vivo with FNR-RFP (a soluble luminal marker). Prior to and after bleaching, *z*-stacks of fluorescent images were collected. Sustained bleaching of a small portion of the *S. neurona* plastid resulted in bleaching of the entire organelle consistent with free marker diffusion through the organelle (Fig. 4C-H; E and H are total projections of the *z*-stacks, a rendered version of this data is available as a movie: see Movie 1 in supplementary material). To ensure that the imaging process itself did not cause excessive bleaching and that the laser provides sufficient spatial precision, *T. gondii* was used as a well-suited control. A *T. gondii* plastid labeled with FNR-RFP was bleached in a vacuole containing multiple tachyzoites. Bleaching was restricted to the single organelle targeted (Fig. 4I-N). Recovery of the fluorescent signal was observed in both *S. neurona* and *T. gondii* plastids over a period of 1 hour (data not shown). Signal recovery probably occurred by import and is consistent with the kinetics of apicoplast targeting in *P. falciparum* (van Dooren et al., 2002) and *T. gondii* (Derocher et al., 2005).

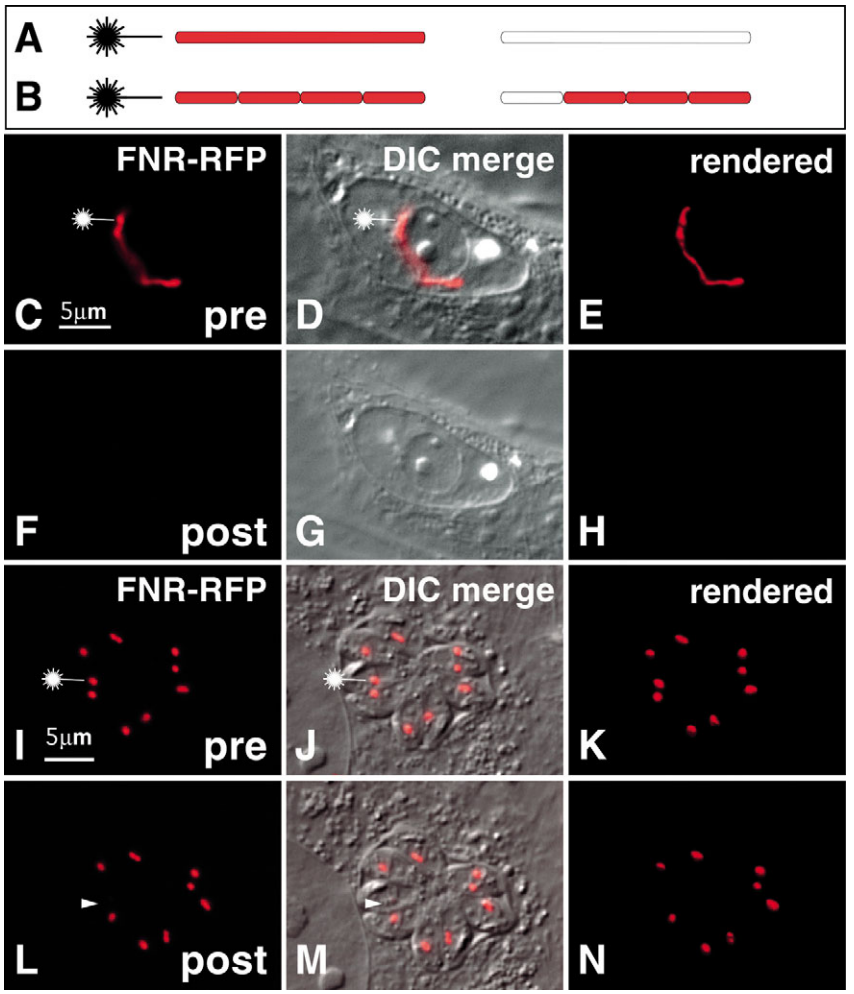

Fig. 4. In vivo laser bleaching experiments show that the *S. neurona* plastid is a continuous organelle. In vivo laser bleaching experiments were performed to test if a fluorescent marker freely diffuses along the entire length of the tubular plastid. The extent of bleaching predicted for organelles with continuous (A) and discontinuous (B) lumen is depicted schematically. FNR-RFP-expressing *S. neurona* (C-H) and *T. gondii* (I-K) parasites were imaged in vivo. Plastids were exposed to a series of short laser pulses at the position indicated by the laser symbol (see Materials and Methods for detail). Cells were imaged before (pre) and after (post) bleaching. (C,F,I,L) Single fluorescence images at the focal plane; (D,G,J,M) merged images of C,F,I and L with the respective DIC image; (E,H,K,N) rendered 3D projection of the entire *z*-stack. (A quicktime movie of these data is available in supplementary material.) Upon exposing the distal end of the *S. neurona* plastid to multiple laser pulses the entire organelle is bleached (F-H). (I-K) Experiments to control for the spatial precision of the laser were performed with FNR-RFP expressing *T. gondii* parasites. (L-N) A single plastid was exposed to the laser resulting in bleaching of only the targeted organelle (white arrowhead) without affecting its nearest neighbors.

Centrosomes and spindles are essential for plastid organization and segregation

In the related parasite *T. gondii*, plastids are associated with the centrosomes during cell division (Striepen et al., 2000). To establish if and when such association occurs in the single tubular plastid in *S. neurona*, infected cultures were triple-labeled with anti-ACP (plastid, green), anti-α-tubulin (spindle, red) and DAPI (DNA, blue). The plastid was found to be in close contact with the nucleus throughout its development. The area of contact between nucleus and plastid coincided with the poles of spindles observed during mitosis and short spindles maintained through interphase (Fig. 3). Double labeling with antibodies against ACP and centrin

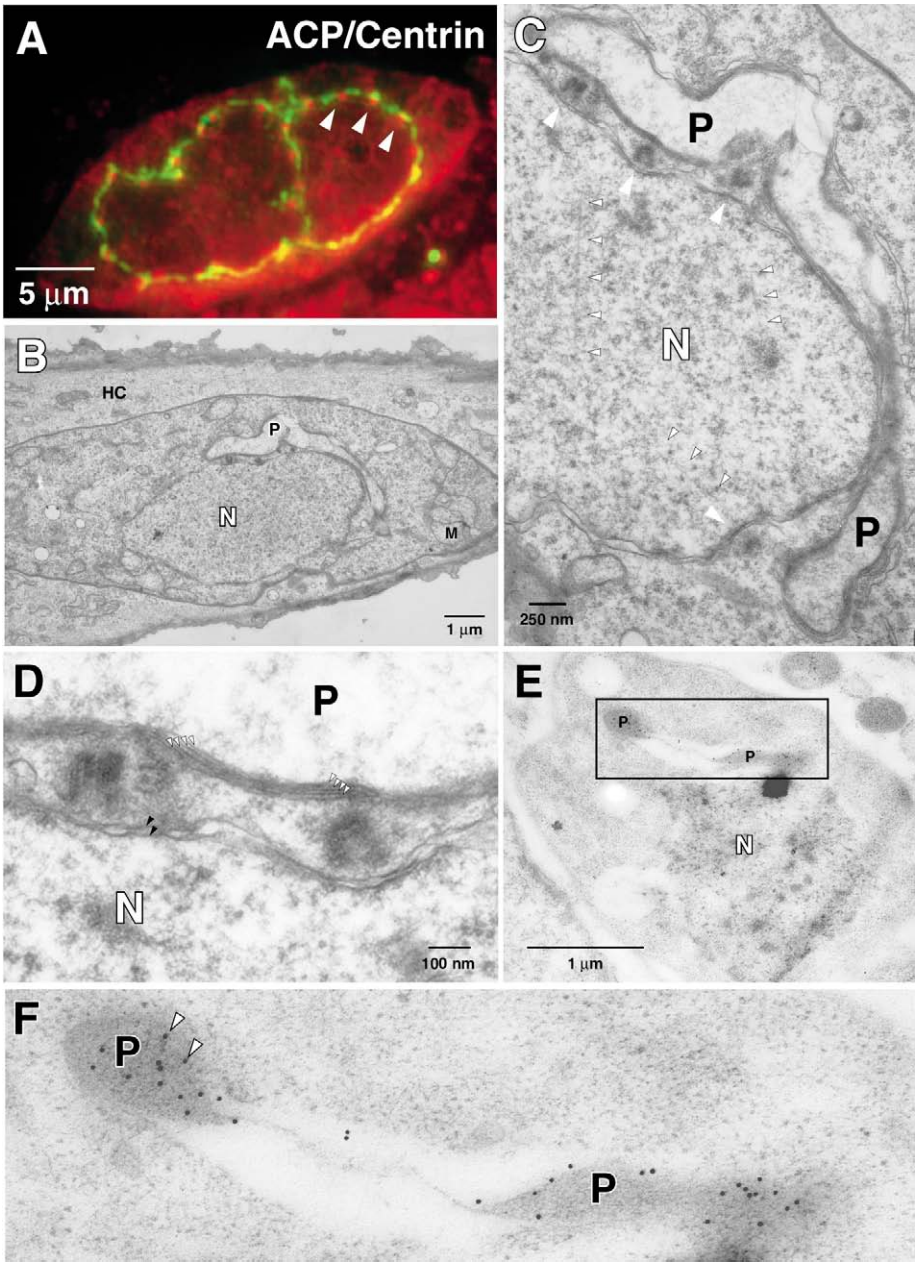

Fig. 5. The tubular plastid shows tight association with centrosomes. (A) Infected cultures were double labeled with antibodies to ACP (green) and centrin (red). Centrosomes (arrowheads) can be seen in association with the tubular plastid. Cultures were fixed in situ, embedded in Epon (B-D) and ultrathin sections were cut parallel to the culture surface and analyzed by electron microscopy. (B,C) Two consecutive serial sections through a developing schizont with its host cell (HC). The nucleus (N) is located in the center of the cell and as seen in a higher magnification (C), four spindle poles (large arrowheads indicate the centrioles) are present. Several intranuclear microtubules (small arrowheads) indicate that this cell is in the early stages of mitosis. Wrapped around the upper right corner of the nucleus is the plastid (P) as a continuous tubular organelle, which is surrounded by four membranes and closely apposed to the centrioles of the centrosome (D, white arrowheads indicate the four plastid membranes; black arrowheads, the two membranes of the nuclear envelope). This organelle is devoid of tubular cristae, which are clearly identifiable on the multiple sections through mitochondria (M). Ultrathin sections were also cut from material that was fixed with formaldehyde and embedded in LR-White resin to preserve antigenicity. Sections were reacted with the ACP antibody followed by an anti-immunoglobulin labeled with 10 nm gold particles. Again a tubular organelle in close proximity to the nucleus was observed (E and enlarged in F) which under this conditions showed heavy and specific gold labeling (arrowheads).

revealed an equally tight association between plastid and centrosomes (Fig. 5A, arrowheads indicate individual centrosomes). To validate this association at higher magnification, *S. neurona*-infected cells were fixed and embedded directly in the tissue culture dish. Blocks were cut and trimmed to preserve the original orientation and sections were then taken parallel to the cell monolayer. Fig. 5B-D shows electron microscope images of serial sections taken through a developing *S. neurona* schizont. A tubular multi-membranous organelle was observed that wrapped around the upper right portion of the central nucleus. At higher magnifications, the four distinct membranes surrounding the plastid were apparent (Fig. 5D). Four centrioles can be identified in Fig. 5C (white arrowheads) that lie in intimate proximity to the plastid [also see Speer and Dubey (Speer and Dubey, 1999)]. To confirm the identification of the organelle as a plastid, *S. neurona*-infected cultures were also fixed and embedded for immunogold labeling. Again a tubular organelle was observed in close proximity to the nucleus. This organelle shows strong and specific labeling for the plastid protein ACP (Fig. 5E,F).

Pharmacological ablation of spindles disrupts plastid organization

If spindles play an important role in plastid organization their disruption should affect plastid morphology. To test this, parasite microtubules were disrupted by treatment with oryzalin. Oryzalin is a dinitroaniline that has been shown to affect both subpellicular and spindle microtubules in Apicomplexa (Morrissette and Sibley, 2002a; Morrissette and Sibley, 2002b). Cultures infected with *S. neurona* were allowed to develop for 36 hours and then treated with 2.5 μg/ml

oryzalin for 24 hours prior to processing for immunofluorescence. A profound loss of plastid organization was observed (Fig. 6C,D). In treated cells, the organelle coiled to the middle of the cell. Even though the organization of the plastid around the nucleus was lost in the drug-treated parasites (compare to untreated control in Fig. 6A,B), centrosome association was maintained. Upon double labeling of drug-treated parasites with anti-centrin and anti-ACP antibody multiple centrosomes were observed associated with the plastid (white arrowheads indicate individual centrosomes in Fig. 6E).

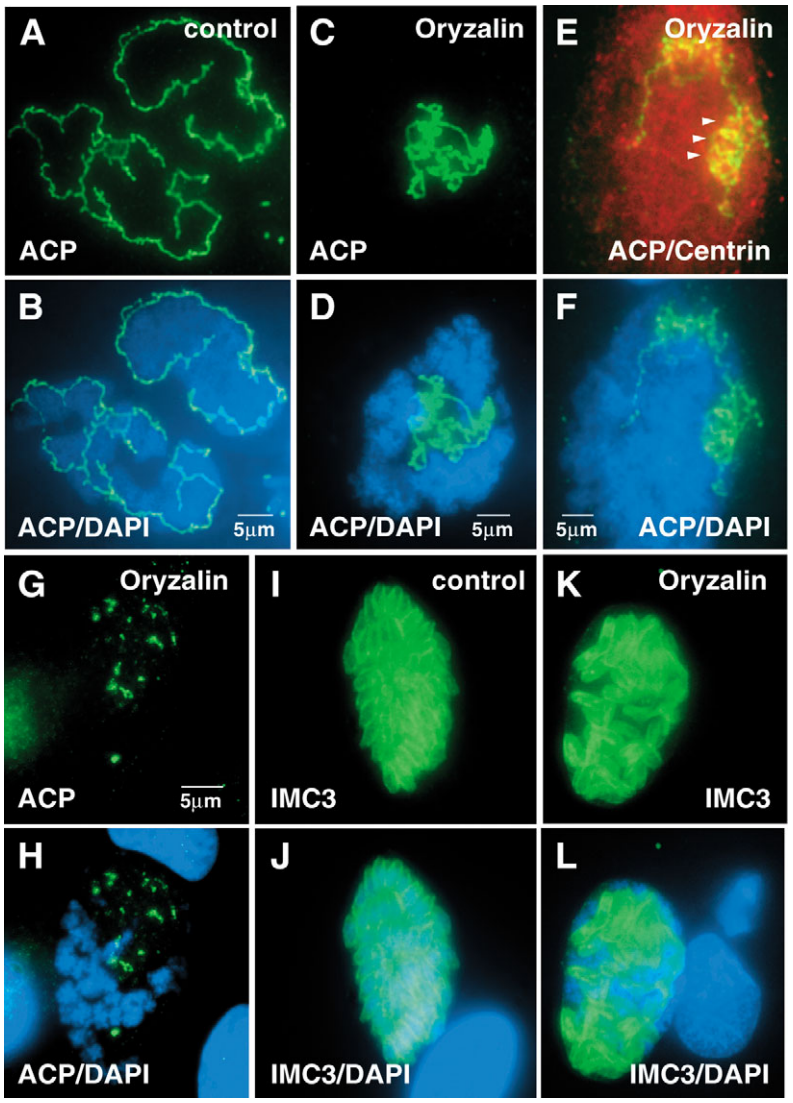

Fig. 6. Ablation of spindles perturbs plastid organization and faithful segregation, but does not prevent fission. (C-F) Infected cultures were allowed to develop for 48 hours and then treated with 2.5 μg/ml oryzalin for 24 hours and stained for plastids using an anti-ACP antibody. (A,B) Untreated controls. The plastid loses its organization and attachment to the nuclear envelope (D,F) but remains associated with centrosomes detected by centrin staining (E). (G,H) After 48 hours of drug treatment plastid fission is observed in some schizonts. (I-L) Labeling of identically treated cultures with an antibody to IMC3 shows that daughter cell budding still occurs (K), however when compared to controls (I,J) treated schizonts seem unable to segregate nuclei and produce anucleate daughter cells (L). (H) Contact of nuclei and plastids is equally lost.

Plastid fission concurs with the last mitosis and daughter cell budding

To endow each daughter cell with a plastid the tubular plastid has to undergo fission. In order to time this event precisely, a molecular marker was used. SnMIC10 is a secretory protein targeted to the micronemes, which probably plays a role in host cell invasion. Importantly, its expression shows tight developmental regulation (Hoane et al., 2003). Fig. 7A shows three consecutive developmental stages of *S. neurona*: a developing schizont (1), a late schizont during budding (2) and a terminal stage schizont showing completed daughter cell formation (3). Expression of SnMic10 is undetectable in the developing schizont (Fig. 5B), but initiates towards the end of the last replication cycle with staining first seen as a dot at mid-cell most probably representing the Golgi or a premicroneme compartment. After completion of daughter cell formation, SnMic10 shows a typical micronemal pattern underlying the apical surface of the merozoite. Plastids were always tubular in the absence of SnMIC10 staining (Fig. 7C,D1), and fission concurred with the beginning of Mic10 expression. This concurrence of plastid fission with the last cell cycle was also evident by triple labeling for plastid, microtubules and DNA (Fig. 7E-H).

To investigate the role of spindles in plastid fission, infected cultures were allowed to develop for 36 hours and then treated with oryzalin for 48 hours prior to processing for immunofluorescence. Plastid fission was evident in the absence of spindles in treated cultures (Fig. 6G). However, these plastids were of unequal size and had lost the nuclear association (Fig. 6H) observed in untreated parasites. We were interested to learn if the observed fission could be a consequence of daughter cell formation in the absence of spindles. For this purpose, infected cultures were treated with oryzalin as described above and labeled with an antibody to *T. gondii* IMC3. IMC3 is a component of the inner membrane complex underlying the parasites plasma membrane, and antibodies to this complex reveal newly forming daughter cells (Fig. 6J) (Gubbels et al., 2004). We observed that drug treatment did not prevent the formation of daughter cells (Fig. 6K,L), however, nuclear segregation and packaging was severely impaired, yielding daughter cells devoid of a nucleus.

Discussion

Plant chloroplasts divide by binary fission and several constrictive rings have been described (Kuroiwa et al., 2002; McAndrew et al., 2001; Vitha et al., 2001). Many of the proteins that make up these rings, and the elements that regulate ring position, are conserved between plastids and their cyanobacterial ancestor (Osteryoung and Nunnari, 2003). By contrast, our previous work in *T. gondii* has indicated that the replication of parasite secondary plastids occurs in association with the centrosomes of the mitotic spindle (Striepen et al.,

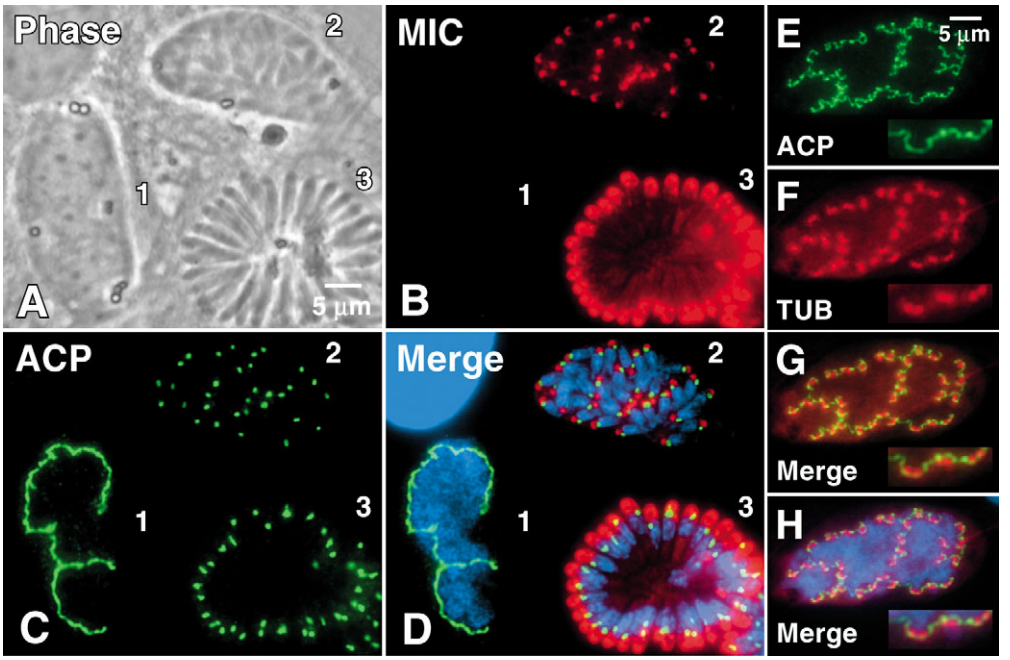

Fig. 7. Plastid fission concurs with the last mitosis and cytokinesis. (A-D) In order to precisely time plastid fission the micronemal protein SnMic10 was used as molecular marker. Infected cultures were fixed 72 hours post-infection and labeled with antibodies to SnMIC10 (red), ACP (green) and DAPI (blue). (A) Three *S. neurona* stages: (1) developing schizont, (2) late schizont initiating budding and (3) final stage schizont with emerging daughter cells. (B) Expression of SnMIC10 coincides with budding and daughter cell formation and is undetectable in developing schizont (see also Hoane et al., 2003). (C,D) In the absence of SnMIC10 expression, plastids are always tubular (D, 1) and plastid fission concurs with the onset of SnMIC10 expression (C). (E-H) Cultures were also triple labeled for plastid, microtubules and DNA. Concurrent with the formation of daughter cell buds (red halos in inset in F), the plastid labeled with anti-ACP antibody starts to fragment (E). Merged images of anti-α-tubulin and anti-ACP staining (G) revealed that plastid spindle pole association is maintained through this last division similar to plastid segregation in *T. gondii* (Striepen et al., 2000). Note that the nuclear DNA is still unsegregated. The emerging fully separated merozoites each contain a nucleus and a plastid (D 3).

2000). The current study shows this to be a conserved mechanism among Coccidia and it might provide a model to understand plastid division in the malaria parasite *Plasmodium*. In *Sarcocystis,* we have found that there is tight association of the plastid with the mitotic spindle and its centrosomes using several molecular markers examined at the light and electron microscopic level. If the mechanism is conserved, why do plastids show such diverse morphology? An obvious difference between *T. gondii* and *S. neurona* are their divergent cell cycle models. In *T. gondii*, the segregation of chromosomes is immediately followed by nuclear division and cytokinesis, and parasites maintain a haploid genome (Radke et al., 2001; Sheffield and Melton, 1968). In *S. neurona*, however, the number of spindles and centrosomes that we observed in growing schizonts suggests that this organism completes six replication cycles prior to daughter cell formation (Fig. 2). The first five cycles involve a succession of chromosomal duplication and segregation accomplished by multiple synchronous spindles throughout the nucleus, but nuclear division and cytokinesis are postponed, resulting in a 32 N nucleus (see Fig. 8 for a schematic outline of this process). The sixth cycle concurs with nuclear segregation and cytokinesis. The surprising persistence of spindles throughout these six replication cycles (with a peculiar 'mini spindle' during interphase) could provide a mechanism organizing chromosomes and organelles in later highly polyploid stages.

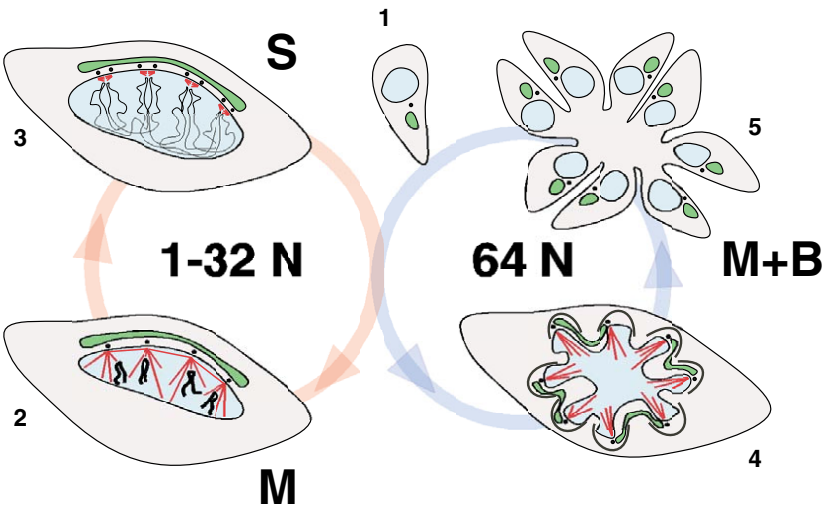

Fig. 8. A schematic outline of the *S. neurona* cell cycle. (1) Merozoites infect a host cell and initiate intracellular development. For 2-3 days the nucleus cycles from mitosis (2) to interphase (3) growing in size and ploidy. Intranuclear microtubular structures are always evident either as full mitotic spindles (2) or as peculiar 'mini-spindles' in interphase (3, constant kinetochore spindle association as drawn, is an attractive hypothesis but has not been experimentally confirmed yet). Concurrent with the last mitosis, budding (4) and cytokinesis (5) occur, giving rise to 64 merozoites (only 8 shown here for simplicity). Plastid (green) development mirrors nuclear (turquoise) events and both organelles are organized by centrosomes (black dots) and spindles (red). S, S phase; M, mitosis; B, budding.

Indeed, pharmacological ablation of spindles results not only in a disorganized nucleus unable to properly segregate during budding, but also a disorganized plastid (Fig. 6). Molecular probes for the identification of centromeres and kinetochores are needed to fully test this model for chromosomes.

It is important to note how closely the development of the plastid mirrors the nuclear events. In *T. gondii*, an ovoid organelle is divided and segregated at the same time as the nucleus in every replication cycle. By contrast, in *S. neurona* we observed a continuous tubular plastid that grows alongside the nucleus (Figs 3, 4 and 5). Organelle continuity was experimentally confirmed in vivo using transgenic parasites (Fig. 5). Plastid fission into 64 individual daughter plastids occurs synchronously with the final nuclear division and segregation thus indicating that plastid fission is timed and regulated in a cell cycle-dependent way. This observation is consistent with a model in which the growing daughter cell pellicle, in conjunction with spindle attachment, could provide the constriction needed for fission (Striepen et al., 2000). An alternative model suggests the action of constrictive rings, similar to those seen in bacteria and plant chloroplasts (Matsuzaki et al., 2001). We have seen no evidence for plastid division rings in *T. gondii* or *S. neurona*, and we have not detected in apicomplexan genomes any of the genes for the conserved proteins associated with these structures (S.V. and B.S., unpublished data). We cannot exclude the possibility that such rings exist and are missed because they are extremely short lived, but they would have to consist of unique molecular components lacking homology to the cyanobacterial division apparatus. If constrictive rings are involved in plastid fission in *S. neurona,* their formation must be controlled in a cell cycle-dependent way and they have to form at multiple defined points along the tubular organelle in a spindle pole dependent-manner.

Spindles are clearly critical for the spatial organization of the plastid during parasite development, but are they required for fission? Ablation of spindles through pharmacological treatment did not prevent fission but broke the coordination of plastid and nuclear division (Fig. 6). Importantly, this treatment leaves intact plastid-centrosome association as well as daughter cell budding. This suggests that these two processes are sufficient for plastid fission and packaging, but that spindles are essential to coordinate this process with nuclear division. This model is in agreement with the observation that spindle ablation in *T. gondii* can lead to the formation of anucleate daughter cells, which in some cases still carry a plastid (Morrissette and Sibley, 2002b). The observation of sustained centrosome association under oryzalin treatment also suggests that this association is not mediated by microtubular structures and mechanisms.

The clarity of the subcellular structure in *S. neurona* when viewed by light microscopy is exceptional among apicomplexan species. This clarity combined with the parasite's peculiar cell cycle makes it a unique model for the cell biological analysis of cell division in Apicomplexa. Transfection technology, as demonstrated in this report, now opens the door to mechanistic studies through genetic manipulation and in vivo analysis.

Funding for this work was provided by grants from NIH-NIAID and additional support from Merck Research Laboratories to B.S., and Amerman Family Foundation and Fort Dodge Animal Health to D.K.H. We thank G. McFadden, S. Salisburry, J. Frankel and J. Gaertig for antibody reagents and Michael White for discussion and critical reading.

References

Colletti, K. S., Tattersall, E. A., Pyke, K. A., Froelich, J. E., Stokes, K. D. and Osteryoung, K. W. (2000). A homologue of the bacterial cell division site-determining factor MinD mediates placement of the chloroplast division apparatus. *Curr. Biol.* **10**, 507-516.

Derocher, A., Gilbert, B., Feagin, J. E. and Parsons, M. (2005). Dissection of brefeldin A-sensitive and -insensitive steps in apicoplast protein targeting. *J. Cell Sci.* **118**, 565-574.

Dinkins, R., Reddy, M. S., Leng, M. and Collins, G. B. (2001). Overexpression of the Arabidopsis thaliana MinD1 gene alters chloroplast size and number in transgenic tobacco plants. *Planta* **214**, 180-188.

Dubey, J. P., Lindsay, D. S., Fritz, D. and Speer, C. A. (2001). Structure of *Sarcocystis neurona* sarcocysts. *J. Parasitol.* **87**, 1323-1327.

Ellison, S. P., Greiner, E. and Dame, J. B. (2001). In vitro culture and synchronous release of Sarcocystis neurona merozoites from host cells. *Vet. Parasitol.* **95**, 251-261.

Fulgosi, H., Gerdes, L., Westphal, S., Glockmann, C. and Soll, J. (2002). Cell and chloroplast division requires ARTEMIS. *Proc. Natl. Acad. Sci. USA* **99**, 11501-11506.

Gao, H., Kadirjan-Kalbach, D., Froehlich, J. E. and Osteryoung, K. W. (2003). ARC5, a cytosolic dynamin-like protein from plants, is part of the chloroplast division machinery. *Proc. Natl. Acad. Sci. USA* **100**, 4328-4333.

Gubbels, M. J., Li, C. and Striepen, B. (2003). High-throughput growth assay for Toxoplasma gondii using yellow fluorescent protein. *Antimicrob. Agents CH.* **47**, 309-316.

Gubbels, M. J., Wieffer, M. and Striepen, B. (2004). Fluorescent protein tagging in Toxoplasma gondii: identification of a novel inner membrane complex component conserved among Apicomplexa. *Mol. Biochem. Parasitol.* **137**, 99-110.

Hoane, J. S., Carruthers, V. B., Striepen, B., Morrison, D. P., Entzeroth, R. and Howe, D. K. (2003). Analysis of the Sarcocystis neurona microneme protein SnMIC10: protein characteristics and expression during intracellular development. *Int J. Parasitol.* **33**, 671-679.

Howe, D. K., Gaji, R. Y., Mroz-Barret, M., Gubbels, M. J., Striepen, B. and Stamper, S. (2005). Sarocystis neurona merozoites express a family of immunogenic surface antigens that are orthologues of the Toxoplasma gondii surface antigens (SAGs) and SAG-related sequences. *Infect. Immun.* **73**, 1023-1033.

Itoh, R., Fujiwara, M., Nagata, N. and Yoshida, S. (2001). A chloroplast protein homologous to the eubacterial topological specificity factor minE plays a role in chloroplast division. *Plant Physiol.* **127**, 1644-1655.

Jerka-Dziadosz, M. and Frankel, J. (1995). The effects of lithium chloride on pattern formation in Tetrahymena thermophila. *Dev. Biol.* **171**, 497-506.

Jerka-Dziadosz, M., Jenkins, L. M., Nelsen, E. M., Williams, N. E., Jaeckel-Williams, R. and Frankel, J. (1995). Cellular polarity in ciliates: persistence of global polarity in a disorganized mutant of Tetrahymena thermophila that disrupts cytoskeletal organization. *Dev. Biol.* **169**, 644-661.

Kuroiwa, H., Mori, T., Takahara, M., Miyagishima, S. Y. and Kuroiwa, T. (2002). Chloroplast division machinery as revealed by immunofluorescence and electron microscopy. *Planta* **215**, 185-190.

Lindsay, D. S., Mitchell, S. M., Vianna, M. C. and Dubey, J. P. (2004). *Sarcocystis neurona* (Protozoa: Apicomplexa): description of oocysts, sporocysts, sporozoites, excystation, and early development. *J. Parasitol.* **90**, 461-465.

Lowe, J. and Amos, L. A. (1998). Crystal structure of the bacterial cell-division protein FtsZ. *Nature* **391**, 203-206.

Lutkenhaus, J. and Addinall, S. G. (1997). Bacterial cell division and the Z ring. *Annu. Rev. Biochem.* **66**, 93-116.

Matsuzaki, M., Kikuchi, T., Kita, K., Kojima, S. and Kuroiwa, T. (2001). Large amounts of apicoplast nucleoid DNA and its segregation in Toxoplasma gondii. *Protoplasma* **218**, 180-191.

McAndrew, R. S., Froehlich, J. E., Vitha, S., Stokes, K. D. and Osteryoung, K. W. (2001). Colocalization of plastid division proteins in the chloroplast stromal compartment establishes a new functional relationship between FtsZ1 and FtsZ2 in higher plants. *Plant Physiol.* **127**, 1656-166.

McFadden, G. I. and Roos, D. S. (1999). Apicomplexan plastids as drug targets. *Trends Microbiol.* **7**, 328-333.

Miyagishima, S. Y., Nishida, K., Mori, T., Matsuzaki, M., Higashiyama,

T., Kuroiwa, H. and Kuroiwa, T. (2003). A plant-specific dynamin-related protein forms a ring at the chloroplast division site. *Plant Cell* **15**, 655-665.
Miyagishima, S. Y., Nozaki, H., Nishida, K., Matsuzaki, M. and Kuroiwa, T. (2004). Two types of FtsZ proteins in mitochondria and red-lineage chloroplasts: the duplication of FtsZ is implicated in endosymbiosis. *J. Mol. Evol.* **58**, 291-303.
Morrissette, N. S. and Sibley, L. D. (2002a). Cytoskeleton of apicomplexan parasites. *Microbiol. Mol. Biol. Rev.* **66**, 21-38.
Morrissette, N. S. and Sibley, L. D. (2002b). Disruption of microtubules uncouples budding and nuclear division in *Toxoplasma gondii*. *J. Cell Sci.* **115**, 1017-1025.
Osteryoung, K. W. and Nunnari, J. (2003). The division of endosymbiotic organelles. *Science* **302**, 1698-1704.
Osteryoung, K. W., Stokes, K. D., Rutherford, S. M., Percival, A. L. and Lee, W. Y. (1998). Chloroplast division in higher plants requires members of two functionally divergent gene families with homology to bacterial ftsZ. *Plant Cell* **10**, 1991-2004.
Paoletti, A., Moudjou, M., Paintrand, M., Salisbury, J. L. and Bornens, M. (1996). Most of centrin in animal cells is not centrosome-associated and centrosomal centrin is confined to the distal lumen of centrioles. *J. Cell Sci.* **109**, 3089-3102.
Radke, J. R., Striepen, B., Guerini, M. N., Jerome, M. E., Roos, D. S. and White, M. W. (2001). Defining the cell cycle for the tachyzoite stage of Toxoplasma gondii. *Mol. Biochem. Parasitol.* **115**, 165-175.
Ralph, S. A., Van Dooren, G. G., Waller, R. F., Crawford, M. J., Fraunholz, M. J., Foth, B. J., Tonkin, C. J., Roos, D. S. and McFadden, G. I. (2004). Tropical infectious diseases: Metabolic maps and functions of the Plasmodium falciparum apicoplast. *Nat. Rev. Microbiol.* **2**, 203-216.
Salisbury, J. L. (1995). Centrin, centrosomes, and mitotic spindle poles. *Curr. Opin. Cell Biol.* **7**, 39-45.
Sheffield, H. G. and Melton, M. L. (1968). The fine structure and reproduction of *Toxoplasma gondii*. *J. Parasitol.* **54**, 209-226.
Sibley, L. D. (2004). Intracellular parasite invasion strategies. *Science* **304**, 248-253.
Speer, C. A. and Dubey, J. P. (1999). Ultrastructure of shizonts and merozoites of Sarcocystis falcatula in the lungs of budgerigars (*Melopsittacus undulatus*). *J. Parasitol.* **85**, 630-637.
Speer, C. A. and Dubey, J. P. (2001). Ultrastructure of schizonts and merozoites of Sarcocystis neurona. *Vet. Parasitol.* **95**, 263-271.
Stokes, K. D. and Osteryoung, K. W. (2003). Early divergence of the FtsZ1 and FtsZ2 plastid division gene families in photosynthetic eukaryotes. *Gene* **320**, 97-108.
Striepen, B., Crawford, M. J., Shaw, M. K., Tilney, L. G., Seeber, F. and Roos, D. S. (2000). The plastid of Toxoplasma gondii is divided by association with the centrosomes. *J. Cell Biol.* **151**, 1423-1434.
van Dooren, G. G., Su, V., D'Ombrain, M. C. and McFadden, G. I. (2002). Processing of an apicoplast leader sequence in Plasmodium falciparum and the identification of a putative leader cleavage enzyme. *J. Biol. Chem.* **277**, 23612-23619.
Vitha, S., McAndrew, R. S. and Osteryoung, K. W. (2001). FtsZ ring formation at the chloroplast division site in plants. *J. Cell Biol.* **153**, 111-120.
Vitha, S., Froehlich, J. E., Koksharova, O., Pyke, K. A., van Erp, H. and Osteryoung, K. W. (2003). ARC6 is a J-domain plastid division protein and an evolutionary descendant of the cyanobacterial cell division protein Ftn2. *Plant Cell* **15**, 1918-1933.
Waller, R. F., Keeling, P. J., Donald, R. G., Striepen, B., Handman, E., Lang-Unnasch, N., Cowman, A. F., Besra, G. S., Roos, D. S. and McFadden, G. I. (1998). Nuclear-encoded proteins target to the plastid in Toxoplasma gondii and Plasmodium falciparum. *Proc. Natl. Acad. Sci. USA* **95**, 12352-12357.
Waller, R. F., Reed, M. B., Cowman, A. F. and McFadden, G. I. (2000). Protein trafficking to the plastid of Plasmodium falciparum is *via* the secretory pathway. *EMBO J.* **19**, 1794-1802.